LHC TRIGGER DESIGN

J.R. Hubbard
DAPNIA/SPP, CEA Saclay
91191 Gif-sur-Yvette, France

Abstract
Trigger issues at LHC are discussed, based on the physics requirements of the experiments. Typical trigger algorithms are presented, as well as full trigger menus and estimated trigger rates. Trigger architectures under consideration for the LHC experiments are compared using very simple 'paper models' based on average values for all system parameters

1 INTRODUCTION

Trigger design and trigger architectures will be discussed in the context of the LHC experiments. These lectures will present a 'top-down' analysis of the LHC trigger requirements and design, based on physics requirements. Level-1 trigger algorithms, which are based on specific trigger hardware, will be described and compared. Higher-level trigger algorithms, based on commercial switching networks and processor farms, will be presented, as well as the expected algorithm execution times. Full trigger menus and expected trigger rates will also be presented. Trigger architectures and implementations under consideration for the LHC experiments will be compared using very simple 'paper models' based on average values for all system parameters. Most of the examples presented in these talks will be based on the ATLAS trigger. I would like to acknowledge the many contributions from my colleagues in the ATLAS trigger/DAQ working groups. Nonetheless, I take full responsibility for the arguments presented here, which do not always reflect the views of the ATLAS community.

2 PHYSICS REQUIREMENTS FOR LHC TRIGGERS

The first step in determining a trigger strategy is to review the physics requirements of the system. This lecture is not meant as a 'physics' lecture. The objective is to review the physics goals to determine which specific trigger algorithms are needed. Inclusive triggers must also be included to provide some coverage for unexpected new physics. A catalog of physics processes for the general-purpose LHC detectors, ATLAS and CMS, including Higgs decays, SUSY particles, gauge bosons, heavy vector bosons, top quarks, and B physics, will be presented. The physics objectives of the specialized detectors, LHC-B and ALICE, will also be discussed.

2.1 LHC machine characteristics

The LHC ring is shown in Fig. 1, with the emplacement of the four LHC experiments - ATLAS, CMS, LHC-B, and ALICE. The interaction energy will be 7 TeV per proton (14 TeV for p-p interactions, 1 PeV for Pb-Pb interactions). The bunch-crossing interval is 25 ns for p-p collisions (40 MHz bunch-crossing rate) and 125 ns for Pb-Pb collisions [1].

The LHC will have a nominal luminosity of 10^{34} /cm^2/s for p-p collisions. The average number of inelastic interactions per bunch crossing will be about 23 at this luminosity. Initial operation will be at lower luminosity ($\leq 10^{33}$ /cm^2/s), with an average of 2.3 minimum-bias interactions per bunch crossing (3.3 interactions including the interaction responsible for the trigger) [2].

The radius of each of the intersecting proton beams will be about 16 μm at collision; the length of the interaction region will be about 5 cm (rms). During the run, the luminosity will degrade as the intensity falls. Each of the experiments will be responsible for monitoring the luminosity and the collision region during the run and during initial beam tuning.

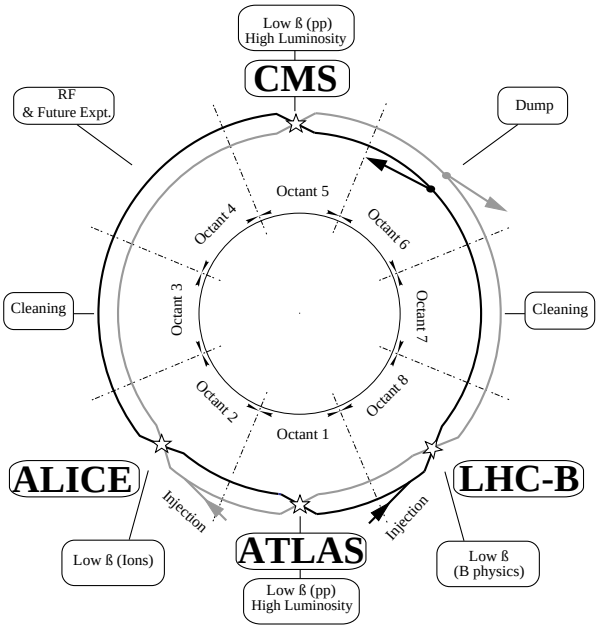

Figure 1: Schematic layout of the LHC

2.2 LHC detectors

ATLAS is a large (diameter 22 m, length 42 m) general-purpose detector with a 2-Tesla solenoidal field in the tracking volume and air-core toroids for the muons. The inner detector consists of precision silicon detectors (pixels and strips) followed by a transition-radiation tracker (TRT) with plastic-fiber and plastic-foil radiators and straw tube detectors. The pulse-height in the TRT can be used to improve the identification of electrons for momenta down to about 0.5 GeV/c. The electromagnetic calorimeters and the forward hadronic calorimeters use liquid argon; the barrel hadronic calorimeters have scintillator readout [3].

CMS is smaller than ATLAS (diameter 15 m, length 30 m, including the very forward calorimeter). The entire calorimeter is inside a 4-Tesla solenoidal field. The iron return yoke provides a second measurement of the momenta of the muons. The inner detector contains silicon pixels and strips and multi-strip gas chambers (MSGCs). The electromagnetic calorimeter is made of lead tungstate crystals. The hadronic calorimeter uses plastic scintillating tiles [4].

LHC-B is a collider experiment designed to study B physics at a constant luminosity of 1.5×10^{32} /cm^2/s, concentrating on particular B decay modes. Characteristic signals include secondary and tertiary vertices and high-P_t leptons and hadrons from B decays. The LHC-B apparatus is a forward spectrometer with a dipole magnet and planar geometry detectors as in fixed-target experiments. The apparatus extends from 10 mrad to 400 mrad in a single arm extending out from the interaction zone. The detector consists of a microvertex detector, a tracking system, aerogel and gas RICH counters for π/K separation, electromagnetic and hadronic calorimeters and a muon system. There will also be small-angle Roman-pot spectrometers in both arms [5].

ALICE is designed to investigate the quark-gluon plasma that is expected to be produced in heavy-ion collisions at the LHC (up to Pb-Pb). Most of the data will be taken at a constant event rate of about 8 kHz (luminosity 10^{27} /cm^2/s for Pb-Pb collisions). Some characteristic signals include prompt photons, J/ψ and upsilon production, and strange particle production. The detector is placed in a weak (0.2-Tesla) solenoidal field, with an inner tracker (silicon plus a cylindrical TPC to measure tracks down to 0.1 GeV/c) surrounded by time-of-flight counters for particle identification. A small-area, high-resolution electromagnetic calorimeter placed under the main apparatus will be used to measure photons. Another small-area detector, placed above the apparatus, will be used to identify

high-momentum particles. One of the forward arms of the detector will be equipped for muon identification [6].

2.3 Physics goals at LHC

The general-purpose detectors, ATLAS and CMS, have similar physics goals, although the detectors have been chosen to have some degree of complementarity in their performance. One clear goal is to find the Higgs boson, or to explore the Higgs sector if a Higgs particle has already been discovered at LEP or at the Tevatron. The next most-likely major discovery could be SUSY particles; SUSY (or supersymmetry) is very popular with particle-physics theorists. Another discovery channel concerns new heavy vector bosons (W′ or Z′), which would be expected in the case of unification beyond the standard model. Other, more exotic, discovery channels, such as leptoquarks, should also be considered. These discovery goals will evolve before the start of the LHC, as more experimental and theoretical results appear.

The LHC will also provide 'bread and butter' subjects, such as top and beauty studies. The LHC will be a top factory, producing millions of tops per year. LHC-B is dedicated to B physics, but the general-purpose detectors will also explore specific B-physics channels. Finally, ALICE will explore the quark-gluon plasma, with nucleon-nucleon interactions at energies of 2.75 TeV/nucleon. The Pb-Pb interactions, at center-of-mass energies of more than 1000 TeV, should exceed the deconfinement threshold and produce conditions similar to the state of the early universe.

Triggers are generally based on the identification of a certain number of trigger objects - photons, leptons, hadrons, and jets. Global quantities such as missing-E_t and total scalar E_t can also be used. Muons are identified by their ability to traverse many interaction lengths of material (typically hadronic calorimeters) without interacting. Photons and electrons, on the other hand, are identified because they are absorbed more easily than hadrons. Quarks and gluons produce jets with electromagnetic and hadronic content. Jets from b-quark fragmentation can be identified by the secondary B-decay vertices ($c\tau$ = 460 μm). Weakly interacting neutral particles (neutrinos or the lightest supersymmetric particle) show up as missing-E_t (non-zero vector sum of all measured P_t). Hadrons can be measured and identified individually (π, K, or proton) by time-of-flight counters (TOF) or by ring-imaging Cherenkov detectors (RICH) in the special-purpose experiments, LHC-B and ALICE.

2.4 The Standard Model

The Standard Model classifies all of the known particles (fermions and bosons) into a symmetry group SU(3)×SU(2)×U(1). This model is consistent with all of the experimental data known today, although it is expected to break down at LHC energies.

The fermion spectrum consists of 3 families of quarks and leptons. Each family has two quarks (with charges +2/3 and -1/3) and two leptons (a lepton with charge -1 and a neutrino with charge 0). The lightest family contains the quarks that make up ordinary matter - the up and down quarks that make up protons and neutrons, and the electron and the electron neutrino. The second family contains the charm and strange quarks and the muon and muon neutrino. The third family contains the top and bottom quarks and the tau and tau neutrino. The top quark was discovered at Fermilab in 1995; it has a mass of about 175 GeV.

The boson spectrum consists of the photon, the gluons (which provide the binding force between the quarks in protons and neutrons), and the vector bosons $W^{\pm}$ and Z^0 (with masses of 80 and 90 GeV, respectively). In order to complete the Standard Model, at least one Higgs boson, which couples to the particle masses, must also exist. One of the main objectives of the LHC program is to discover the Higgs boson.

The B-physics goals of the general-purpose detectors, ATLAS and CMS, include the study of CP violation, B_s^0 mixing and rare decay modes. The decay modes $B_d^0 \rightarrow J/\psi\ K_s^0$, $B_d^0 \rightarrow \pi^+\ \pi^-$, and $B_s^0 \rightarrow J/\psi\ \varphi$ can be used to constrain the three angles β, α, and γ, respectively, of the unitary triangle. B_s^0 mixing can be studied in the decay $B_s^0 \rightarrow D_s^-\ \pi^+ \rightarrow \varphi\ \pi^-\ \pi^+$. One rare decay mode that can be studied easily is $B_s^0 \rightarrow \mu^+\ \mu^-$ [7-10].

LHC-B is specifically designed for B physics. A large number of exclusive decay modes will be studied, with branching ratios down to 10^{-8} or smaller. A major objective is the study of CP-violation in rare decay modes. The major advantages of the LHC-B experiment are the forward geometry, allowing larger Lorentz boosts and better proper-time measurements, and the π/K separation obtained from ring-image Cherenkov counters, allowing additional flavor tagging [11].

The LHC will be a veritable top factory, producing 6000 $t\bar{t}$ pairs per day even at a very low initial luminosity of 10^{32} /cm^2/s. This will allow a precise measurement of the top mass in the mode $t\bar{t} \rightarrow (b\ W^+)\ (b\ W^-) \rightarrow (l^{\pm}\ \nu\ b)\ (j\ j\ b)$. Study of single top production is also important. In addition, searches will be performed for rare decay modes such as $t \rightarrow b\ H^+$ or $t \rightarrow c\ Z$.

The initial design of ATLAS and CMS was strongly influenced by the requirement of observing the decays of the Standard Model Higgs. The preferred decay modes were $H^0 \rightarrow \gamma\ \gamma$ for a light Higgs, $H \rightarrow Z\ Z^* \rightarrow 4$ leptons for intermediate masses, and $H \rightarrow Z\ Z$ or $W\ W$ for high-mass Higgs [12]. Now theorists give little credence to the Standard Model Higgs, and there is more emphasis on the need for broad physics discovery potential rather than excellent acceptance and/or resolution for a single favored discovery channel.

2.5 Grand unification

The Standard Model has three coupling constants - two for the unified electro-weak interaction, and one for the strong color interaction. There is considerable hope that these coupling constants will merge into a single grand unification coupling constant at an energy below the Fermi energy (10^{19} GeV). Any new symmetry group, corresponding to the partial or total unification of these three forces, will result in at least one new neutral vector boson, Z'. The Z' should be easily visible, through its leptonic decays, as a high-mass peak in the dilepton mass spectra.

2.6 Supersymmetry

Supersymmetry was proposed as a means of resolving the 'hierarchy' problem: The normal particle mass spectrum includes vector bosons with masses of about 100 GeV, and very heavy objects with masses of about 10^{15} GeV. Theorists cannot understand how this is possible unless there are important cancellations among the contributions to the masses of the lighter particles. The radical proposal for accomplishing this was to invent a new boson for every known fermion, and a new fermion for every known boson. If the masses of these new particles were below a value of about 1 TeV, the necessary cancellations would occur because of a sign difference between the fermion couplings and the boson couplings. The new particles are named after their Standard Model partners; the particles and their intrinsic spins are given below:

Standard Model particles		**Supersymmetric particles**	
leptons	J=1/2	sleptons	J=0
quarks	J=1/2	squarks	J=0
gluon	J=1	gluino	J=1/2
photon	J=1	photino	J=1/2
W, Z	J=1	wino, zino	J=1/2
Higgs	J=0	higgsino	J=1/2
graviton	J=2	gravitino	J=3/2

The wino will mix with the charged higgsino to form particle states now called Charginos, and the photino will mix with the zino and the neutral higgsinos to form Neutralinos.

The Higgs sector in supersymmetry (SUSY) contains a minimum of 5 Higgs particles: h^0, H^0, A^0, H^+, H^-. To first order, the h^0 should be lighter than the Z^0, and the H^0 should be heavier than the Z^0. After radiative corrections to the h^0 mass, it could be somewhat heavier than the Z^0. The Higgs masses and couplings and their decay modes are essentially determined by two parameters in the minimal version of supersymmetry (MSSM) [13]. Since the Higgs particles couple to mass, decays to heavy particles such as τ leptons and b or t quarks are favored. Some of the dominant decay modes are expected to be: $H^+ \rightarrow \tau^+\nu$; $A^0 \rightarrow \tau^+\ \tau^-$; $h^0 \rightarrow b\ \bar{b}$; $H^0 \rightarrow h^0\ h^0 \rightarrow b\ \bar{b}\ b\ \bar{b}$. In much of parameter space,

$b\bar{b}\ H^0 \rightarrow b\bar{b}\ b\bar{b}$ final states would be dominant. The characteristic Higgs coupling to mass would be established if tau decay modes were shown to be more frequent than electron and muon decays; in all other interactions, lepton universality is expected. The ratio of $\tau^+\tau^-$ decays to $b\bar{b}$ decays is predicted to be about 10% for Higgs decay. The scalar Higgs could be distinguished from vector bosons such as Z or Z′ if the decay mode $H^0 \rightarrow \gamma\gamma$ could be established. The measurement of the different Higgs decay modes (or their upper limits) could be used to fix the parameters of the SUSY model.

The most convincing way to discover SUSY, and perhaps the most simple, would be to observe the SUSY particles themselves. The cross sections should be large, and SUSY particles could be discovered very early in the LHC operation. SUSY particles are expected to be produced in pairs, and to decay to final states containing at least one SUSY particle. The lightest of the SUSY particles is expected to be neutral and stable; it would escape from the detector without interacting, leaving missing energy in the event. This missing energy is expected to be the dominant feature of SUSY events. Another important feature is the presence of high-P_t leptons coming from cascade decays of the higher-mass SUSY states. The higher-mass neutralinos and charginos would decay into the lower-mass members, emitting a photon, W*, Z*, or Higgs. The W* or Z* would decay into leptons or jets, and the Higgs would decay mainly into b jets. The scalar-E_t (the scalar sum of the E_t in the event, or, alternatively, the sum of the E_t in all of the jets in the event) would also tend to be large. Missing-E_t, scalar-E_t, photons, multiple leptons, multiple jets, and b jets should all be considered as possible SUSY signatures.

2.7 Quark-gluon plasma in ALICE

ALICE, A Large Ion Collider Experiment, is designed to probe the quark-gluon plasma (QGP) in its asymptotically free ‘ideal gas’ form. The central rapidity region will have a very large number of particles with momenta close to the QCD energy scale (hadronic temperature) of 200 MeV. The number of particles in the Pb-Pb interactions can be up to 1000 times higher than in normal LHC p-p interactions. The characteristics of these events can be used to probe the parameters of the quark-gluon plasma: Charm production rates can be used to determine parton kinematics in the early stage of the plasma. Prompt photons will reveal the temperature of the plasma. J/ψ and upsilon production will probe deconfinement. Strange particle production will give indications on the phase transition ending the quark-gluon plasma. All of these signals will be measured in the ALICE experiment.

2.8 Background

The main background in the LHC experiments will come from the interaction zone itself. Background arising from dijet production through hard interactions (QCD) will dominate most of the trigger rates. Nonetheless, background from new physics itself cannot be neglected. Top production will produce major background in many of the new physics searches because of its high rate and because the top decay products, b and W, are signatures for many of these searches. SUSY will be an important new discovery if it is found, but the great variety of SUSY final states will provide background to the more exclusive SUSY searches.

Background from cosmic rays will be negligible compared to the signals coming from the interaction zone. On the other hand, beam halo could produce events faking large missing-E_t, and the general radiation level (low-energy photons and neutrons) could help produce fake muon triggers. The fake muons will be eliminated easily by the Level-2 track match. The fake missing-E_t may require special algorithms in the higher-level triggers.

3 TRIGGER DESIGN AND TRIGGER ARCHITECTURES

The LHC triggers must be designed to meet the challenge of this vast physics program. The key to a successful trigger is flexibility. This lecture will present various trigger strategies for the LHC experiments. Trigger hardware - buffers, switching networks, interfaces, processor farms, and supervisors - will be discussed, as well as the possible use of regions-of-interest and preprocessing.

3.1 Trigger evolution at the TeVatron

The Tevatron experiments, CDF and D0, were designed to do high-P_t physics, assuming that they would not be able to do competitive B-physics. The first-level triggers did not include tracking data. Nonetheless, CDF learned that they could indeed do good physics with $B-\overline{B}$ events. D0 could not follow this action, because the D0 apparatus had no magnetic field in the tracking volume. Now both experiments are preparing upgrades to their tracking systems and their triggers to try to improve their B-physics capabilities; D0 is also adding a solenoidal magnetic field for the tracking volume.

3.2 Trigger strategies at LHC

The ATLAS trigger system is shown in Fig. 2. Level 1 reduces the rate from the 40 MHz bunch-crossing rate to 100 kHz or less for transfer to the Level-2 readout buffers (ROBs). Then the combined Level-2 and Level-3 selections reduce the event rate to a level that can be written to permanent storage (about 100 MB/s or 100 Hz of full events). At Level 1, calorimeter and muon data are treated separately (with reduced granularity) in special-purpose processors. At Level 2 and Level 3, full granularity data, including tracking data, are treated in commercial processor farms.

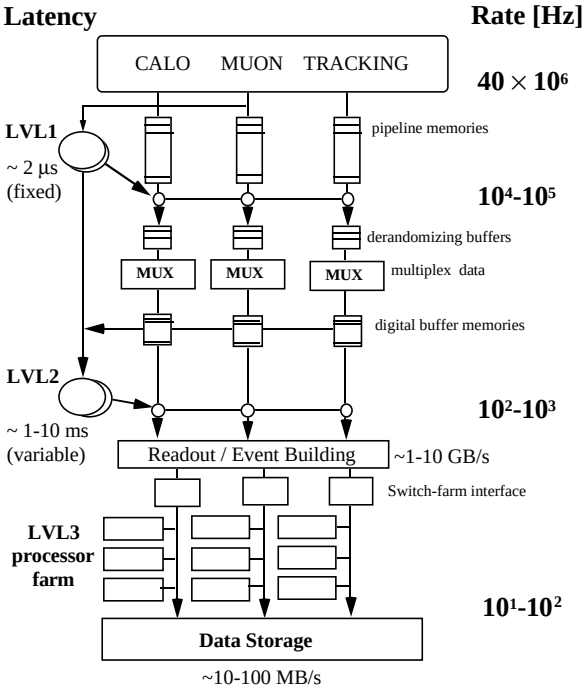

Figure 2: ATLAS trigger system.

The ATLAS design has separate Level-2 and Level-3 processor farms; the data-transfer bandwidths into Level 2 and Level 3 are comparable, because only data from Regions of Interest (RoIs) identified by the Level-1 trigger are transferred to the Level-2 processors. The CMS design is more ambitious: a single processor is used for (the virtual) Level 2 and for Level 3, and the RoI concept is not used.

The current LHC-B trigger design, shown in Fig. 3, has four levels of trigger [14]. Parallel Level-0 triggers select high-P_t muon, electron, and di-hadron candidates in the muon and calorimeter systems. The Level-0 trigger also has a pileup veto, designed to select bunch-crossings with a single interaction by rejecting events with large energy deposit in the calorimeters (2.2 TeV or more). Level-1 consists of a hardware track/vertex trigger with a maximum latency of 50 μs. Level-2 and Level-3 algorithms are performed in a processor farm. The average event size at LHC-B is about 100 kB, and

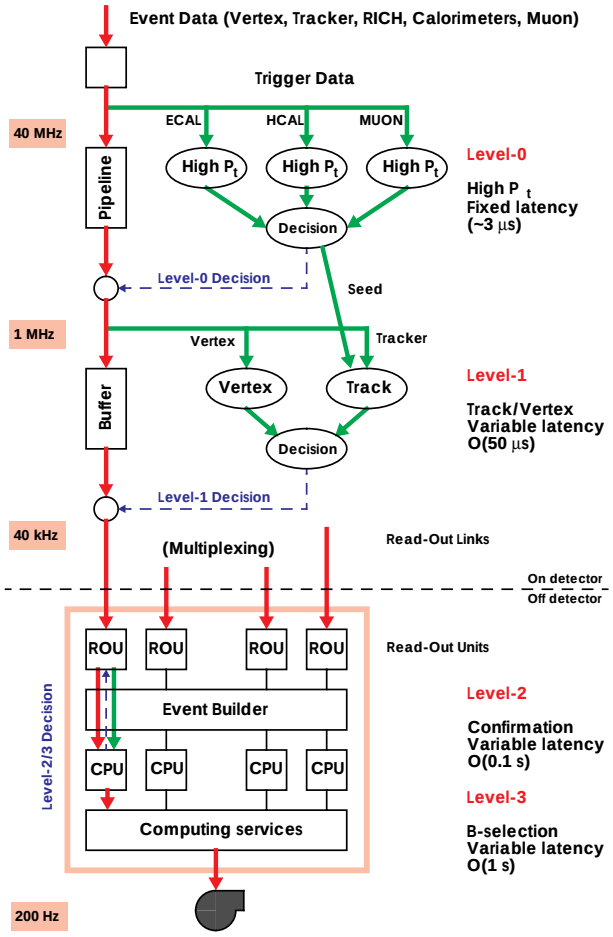

Figure 3: LHC-B trigger system.

the maximum trigger rates are 1 MHz at Level 0, 40 kHz at Level 1, and 200 Hz after Level 2 and Level 3.

The ALICE trigger design must take into account the very low beam luminosity planned for the nucleon-nucleon interactions. The event rate in the TPC is limited to about 8 kHz. A Level-0 analog track-multiplicity trigger, with a latency of 1.2 μs, will be used to signal bunch-crossings with an interaction (roughly one in a thousand). The Level-1 trigger, with a latency of 2.4 μs, is based on muon and calorimeter data, in addition to the multiplicity signal. The Level-2 trigger uses the data from the silicon detectors and the TPC in specific processors with latencies limited to 100 μs to apply more selective algorithms, such as mass cuts. The Level-2 trigger will also provide past and future protection to ensure that there is a single interaction present in the TPC. After event-building, further data reduction will be realized in the commercial processors responsable for logging the selected events to permanent storage.

3.3 Level 1 trigger hardware at ATLAS and CMS

The maximum latency for the Level-1 ATLAS and CMS triggers is 2-3 μs. Special-purpose pipe-lined ASICS are used to make these decisions. The Level-1 output rate is limited by the bandwidth of the optical-fiber links between the frontend readout drivers (RODs) and the readout buffers (ROBs). Typical design calls for 1 Gb/s optical links input to each of the ROBs. Current ATLAS and CMS trigger designs allow for a maximum Level-1 output rate of 100 kHz. The frontend design is critical to the Level-1 trigger performance because it cannot be upgraded easily.

Tracking data are not used for the Level-1 triggers. The muon data come from special trigger chambers with good time resolution, allowing bunch-crossing identification. The muon trigger primitives are muon candidates with P_t above one of the muon trigger thresholds. The calorimeter data consist of sums over trigger towers ($\delta\eta \times \delta\varphi$ = 0.1x0.1 for ATLAS, 0.087 for CMS). The

calorimeter trigger primitives consist of electron/gamma candidates with narrow energy deposits in the electromagnetic calorimeter and very little energy in the hadronic calorimeter, jet candidates with broader energy deposits in both the electromagnetic and the hadronic calorimeters, and missing-E_t calculated by summing E_t over the full calorimeter (out to $|\eta| \approx 5.0$). Single-hadron and tau-jet candidates can also be identified in the calorimeter, and the total scalar E_t sum can be calculated.

The Central Trigger Processor counts the number of muon, electron/gamma, hadron/tau, and jet candidates in the event, and makes a global Level-1 trigger decision based on the number of candidates of each type passing different P_t thresholds. The missing-E_t and the scalar-E_t can also be used in the global Level-1 trigger decision.

3.4 Data flow in higher-level triggers

All data for events accepted by the Level-1 trigger are stored in the ROBs for use by the higher-order triggers (Level 2 and Level 3). The data are stored in paged memory so that events can be deleted out-of-order without fragmenting the available buffer space. The buffer space must be large enough to accommodate the average Level-2 latency, estimated to be greater than 10 ms.

The ROBs are connected to the Level-2 processors by means of a switching network. The total bandwidth into the ROBs is about 100 kHz $\times$ 1 MByte = 100 GB/s. This bandwidth would be difficult to handle on standard commercial switching networks. The solution to this problem is to transfer only a small part of the data to the Level-2 processors. Different trigger architectures have been studied at ATLAS and at CMS, corresponding to different trigger strategies. ATLAS achieved an important reduction in the data volume by selecting Regions of Interest (RoIs) based on the information from the Level-1 trigger. CMS reduced the data volume by selecting only calorimeter and muon data for the first round of Level-2 algorithms. Current thinking in both experiments would be to combine these features, using both RoIs and sequential processing to reduce the overall data-transfer bandwidth to a few GB/s.

The Level-2 latency and the number of processors required can be reduced if the data transferred to the processors is well-suited to the needs of the Level-2 algorithms. Ideally, the data can be prepared in the RODs before their transfer to the Level-2 ROBs. If further treatment is needed, it can be performed by processors resident in the ROB modules or in the interface between the ROBs and the switching network. Examples of preprocessing that could improve the trigger performance include the calculation of energy sums for the jet triggers and the determination of space points in the silicon trackers.

The ATLAS trigger is designed for a Level-2 accept rate of up to about 1 kHz. All data for these accepted events are transferred to the Level-3 processors, which use a form of the off-line reconstruction programs to refine the rejection, perform calibration and alignment functions, classify the events into physics categories, and perform fast-lane physics analysis. The data-transfer bandwidth into the Level-3 processors is about 1 GB/s at 1 kHz, comparable to the rate of RoI data into Level 2.

The switching network connects the ROBs to the Level-2 and Level-3 processors. Current ATLAS and CMS designs call for 1000 to 2000 ROBs and several thousand processors. Switches with thousands of ports are not yet available commercially; on the other hand, the bandwidth available from individual ports is much higher than the requirements for a single ROB or a single processor. The number of ports can be reduced by grouping the data from several ROBs in a ROB-to-Switch Interface (RSI), and grouping several processors into a subfarm served by a Switch-to-Farm Interface (SFI). The intelligence in the RSIs and the SFIs can be used to code and decode messages and to reformat and reorder the data. Current thinking at ATLAS and CMS favor switches with 500 to 1000 bi-directional ports. Candidates for the switching networks include ATM, DS-link, Fiber Channel, and SCI.

3.5 Processing schemes for higher-level triggers

The trigger architecture described in the ATLAS Technical Proposal (see Fig. 4) called for separate local processor farms and switching networks for each of the subdetector systems, plus a global switching network and a global Level-2 processor farm. The local/global partition was intended to

reduce the Level-2 latency by allowing feature extraction in parallel for different subdetectors and for different RoIs. In this model, the Level-3 trigger system required a separate switching network to connect all of the ROBs to the Level-3 processor farm.

An alternative architecture has been proposed for the ATLAS trigger with a single Level-2 processor farm and a single switch [15]. This architecture, which is identical to that of CMS, facilitates the access to the event data, and thus simplifies the implementation of a sequential event selection strategy. Certain events can be rejected very early using a small amount of data from the calorimeter and muon systems. The more complex tracking algorithms are executed only for the fraction of events that pass these initial selection criteria. The Level-3 processors can be attached to the same switching network, and the implementation of different algorithms at Level 2 (partial data) or at Level 3 (full data) can be optimized. In CMS, the same processor is used for the Level-2 and Level-3 algorithms.

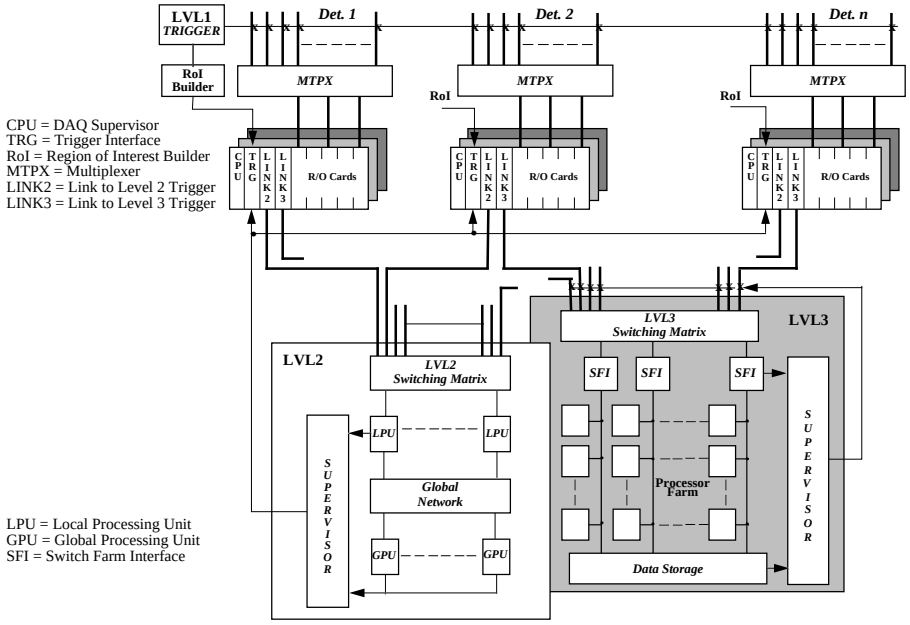

Figure 4: Local/global processing in ATLAS Technical Proposal model.

'Push' and 'pull' data flow scenarios have been envisaged for the ATLAS Level-2 trigger. In the 'push' scenario, a supervisor selects a processor, then tells each of the relevant ROBs to send data to the selected processor; any further data requests must be addressed once again to the supervisor. In the 'pull' scenario, the supervisor selects a processor, which then requests data from the ROBs as needed. The sequential selection algorithms are simplified in the 'pull' scenario, because the supervisor intervenes only at the beginning and at the end of the event analysis.

In order to increase the physics potential of the trigger system, some time-consuming Level-2 trigger algorithms can be executed partially or completely on special FPGA processors. The partial execution of an algorithm corresponds to a preprocessing function. One possible use of a FPGA processor would be for the TRT full scan algorithm required for the selection of B-physics candidates. This algorithm searches for tracks in the full tracking volume and takes much longer than tracking algorithms based on RoIs. The execution time can be reduced by performing the track-finding part of the algorithm on the FPGA processor, while leaving the track fitting to be done on the general-purpose Level-2 processors.

3.6 Supervisor specifications

The Level-2 supervisor receives RoI data for each event accepted at Level 1 and assigns the Level-2 processors for the event. In the case of a 'push' data flow, all relevant ROBs are instructed to send their data to the selected processor(s). In the case of a 'pull' data flow, the list of RoIs is sent to the processor assigned to the event, and the processor requests data from the ROBs as needed.

The supervisor also receives the final decisions from the Level-2 processors, and distributes them to all of the Level-2 ROBs. In order to avoid a high rate of very short messages, a certain number of decisions are collected by the supervisor before sending them to the ROBs in a single packet. A 'broadcast' or 'multicast' transmission can be used if it is available in the switching network protocol.

3.7 Level 3 trigger strategies

Level 3 functions include final event selection, calibration and alignment, event filtering (assigning events to different data streams for off-line processing), and fast-lane physics analysis (looking for 'gold-plated' signals such as $H \rightarrow Z^0 Z^0 \rightarrow 4$ leptons, or $B^0 \rightarrow J/\psi K^0$). The Level-3 system should also be capable of signalling certain unusual events to the shift leader for immediate study and performing an automated search for deviations in certain distributions (masses and missing-E_t).

In the Technical Proposal version of the ATLAS trigger, the input rate to the Level-3 processors was about 1 kHz, and the output rate was about 100 Hz. But many of the algorithms foreseen for Level 3 could, in fact, be executed at Level 2 with shorter execution times (more highly optimized code) and with much smaller data transfers. The extra processing power liberated by this trigger strategy could be used to increase the overall physics potential of the trigger system (higher rates for complex algorithms and/or increased physics analysis at Level 3).

4 TRIGGER SIMULATIONS

Trigger simulations are needed to determine trigger rates and trigger efficiencies. This lecture will describe the main tools available for trigger simulations at LHC. The high-P_t trigger algorithms foreseen for the LHC experiments will be described. Rates will be presented for inclusive muon, electron/gamma, jet, and missing-E_t triggers as a function of threshold, at low luminosity (10^{33}) and at high luminosity (10^{34}).

4.1 Event generation

A major goal of any trigger strategy is to obtain high, measurable efficiencies for a certain catalog of anticipated physics processes, without exceeding the design trigger bandwidths. The LHC triggers are based on the identification of certain trigger objects - muons, electrons, photons, hadrons, jets, and missing-E_t. Trigger rates at the LHC are generally determined by background from the interaction region. For most LHC triggers, the background events are 'minimum bias' dijet events.

Single particles and full events can be generated using an event generator such as PYTHIA or ISAJET. Single particles are used to measure efficiencies for each of the trigger objects. Dijet events are used to measure trigger rates. Physics events can be generated to determine the trigger efficiency for specific channels of interest. Event generation is very rapid, allowing thousands of events to be simulated on a single machine overnight. ATLAS has already simulated several million dijet events as part of a 10-million event simulation project.

The response of the experimental apparatus can be studied using the GEANT simulation program. The full detector geometry, particle interactions in the detector material, and signals produced in the active elements can be simulated. Multiple beam interactions can be included. GEANT is the usual tool for testing the adequacy of a particular detector design. Simulation of a single event requires a large fraction of an hour on today's UNIX machines, and very large samples of dijet events are required to simulate the LHC trigger rates. The time required can be reduced by filtering the PYTHIA output to select events compatible with selected trigger conditions before processing them through the full GEANT simulations.

Many useful studies can be performed using fast simulation programs instead of the full GEANT simulations. Fast simulation programs use parameterized distributions to replace some of the detailed interactions of the individual particles in an event. The fast simulations nonetheless take into account the material in the tracking volume, the transverse and longitudinal distribution of the energy deposit in the calorimeters, pulse shaping, and pile-up. The fast simulations are performed in individual energy bins for the hard interactions in PYTHIA, then the results are added together with weights appropriate to each energy bin [16].

4.2 Muon triggers

The ATLAS Level-1 muon trigger in the barrel region is illustrated in Fig. 5. The Level-1 trigger uses signals from fast Resistive Plate Chambers (RPC) to measure the muon P_t and time-stamp the bunch crossing. Low-P_t triggers require three-out-of-four hits in the inner RPCs, and high-P_t triggers require a low-P_t trigger plus two-out-of-three hits in the outer RPCs. Three trigger thresholds are available for the low-P_t trigger, and three more for the high-P_t trigger [17].

The Level-2 muon trigger uses the trigger chambers to determine roads in the precision muon chambers (Monitored Drift Tubes). The MDTs determine η, φ and the sagitta for each muon

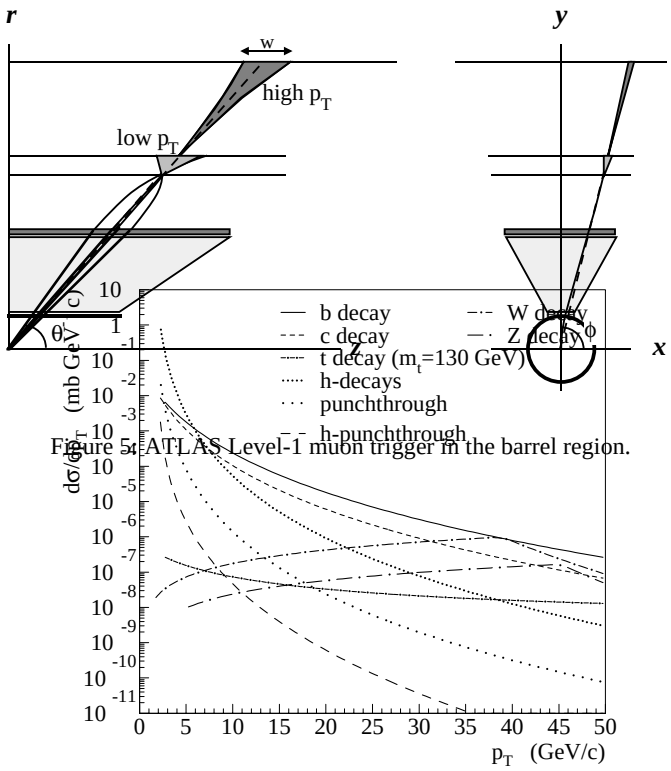

Figure 5: ATLAS Level-1 muon trigger in the barrel region.

Figure 6: Sources of muon triggers (|η|<3).

candidate. The precision muon momentum determination is performed by interpolation in a Look-Up Table, so that the complicated field integrals do not have to be calculated for each track [18].

The muon trigger should be dominated by real muons from beam interactions. The shielding has to be designed carefully to avoid saturating the muon trigger with fake tracks due to background radiation. The sources of muon triggers are shown in Fig. 6. For P_t thresholds of 6 GeV/c or higher, muons coming from heavy quarks (b,c) are more frequent than muons from light quarks (u,d,s). The major known source of dimuons above 20 GeV/c is $Z^0 \rightarrow \mu^+ \mu^-$ decay.

4.3 Electron/gamma triggers

The Level-1 e/γ trigger for ATLAS is based on trigger towers with $\delta\eta \times \delta\varphi = 0.1 \times 0.1$. Analog signals are added to obtain the trigger tower energy sums. The e/γ trigger requires electromagnetic E_t above threshold in any two adjacent trigger towers. Electromagnetic isolation cuts apply to the outer 12 towers in a 4×4 tower region about the signal towers. Hadronic isolation cuts apply to the 16 hadronic cells in this same 4×4 tower region [3]. The original e/γ trigger algorithm favored two of the four two-cell combinations in the center of the 4x4-tower region [19]. This algorithm was intrinsically charge-asymmetric due to the asymmetric distribution of bremsstrahlung radiation from electrons and positrons [20]. The current algorithm is charge symmetric.

The Level-1 e/γ trigger for CMS is based on towers which are slightly smaller than the ATLAS towers. CMS uses digital signals to make the energy sums. The EM isolation energy is the smallest of the energy sums formed about each of the four corners of the central EM tower. Separate hadronic cuts concern the single tower behind the central EM tower, and the 8 towers surrounding the central tower. The CMS Level-1 trigger includes a single-bit fine-grained EM trigger tag at Level 1. This provides the possibility of a low-P_t 'non-isolated' (or partially isolated) electron trigger which can be used to enhance the trigger for top and B physics [21].

The Level-2 e/γ triggers use the full granularity of the electromagnetic calorimeters to improve the e/γ identification. Shape factors are tested to verify that the candidates have the narrow shape expected for photons or electrons. The shape factors take account of the spread in ϕ due to bremsstrahlung radiation. Electrons are separated from photons by requiring a track in the inner detector that matches the E_t, η, and ϕ measured in the calorimeter. In ATLAS, the electron signal in the TRT can also be used to improve the rejection of background from single charged hadrons. The Level-2 trigger rates for isolated electrons and gammas, shown in Fig. 7 for high luminosity, were obtained from full GEANT simulations of the ATLAS trigger [22,23]. The rates shown correspond to 80% efficiency for electrons or photons at the nominal P_t threshold. The trigger rates at high luminosity (10^{34} /cm^2/s) are more than ten times the trigger rates at low luminosty (10^{33} /cm^2/s) because the trigger cuts are less efficient in the presence of minimum-bias background.

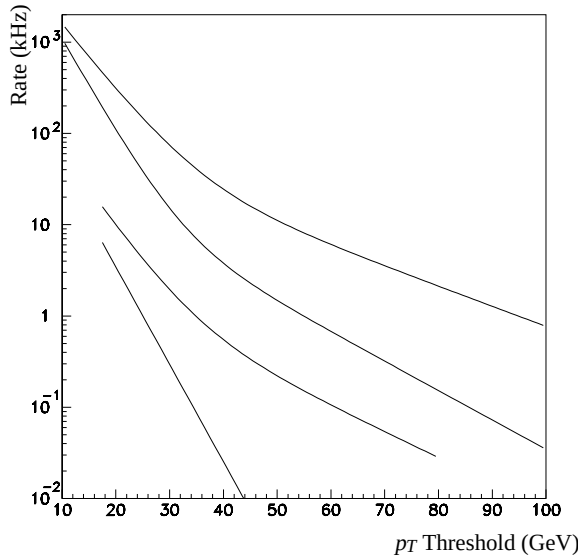

Figure 7: Electron and gamma trigger rates at high luminosity. Starting from the bottom, the curves represent Level-2 electron and gamma trigger rates, then Level-1 EM cluster rates with and without isolation cuts.

4.4 Jet triggers and missing-E_t

ATLAS and CMS have studied similar Level-1 jet trigger algorithms. CMS prefers a non-overlapping 4x4-tower jet algorithm [4,21], whereas most of the ATLAS studies have concentrated on the 8×8-tower algorithm with overlapping windows [24]. For the higher-E_t jets, the threshold is, of course, sharper for the 8×8-tower algorithm. On the other hand, a smaller window would be preferable for lower-E_t jets. Dijet decays of W's and Z's could be found most easily using small, overlapping jet windows.

Jet trigger rates at low luminosity ($L=10^{33}$ /cm^2/s) are shown in Fig. 8 for the ATLAS trigger. An average of 1.8 minimum-bias events have been added to each dijet event. Trigger rates are shown for one, two, three and four jets above the trigger threshold. These trigger rates were found using a fast simulation program [16].

The jet trigger rates at high luminosity are shown in Fig. 9, where 18 minimum-bias events

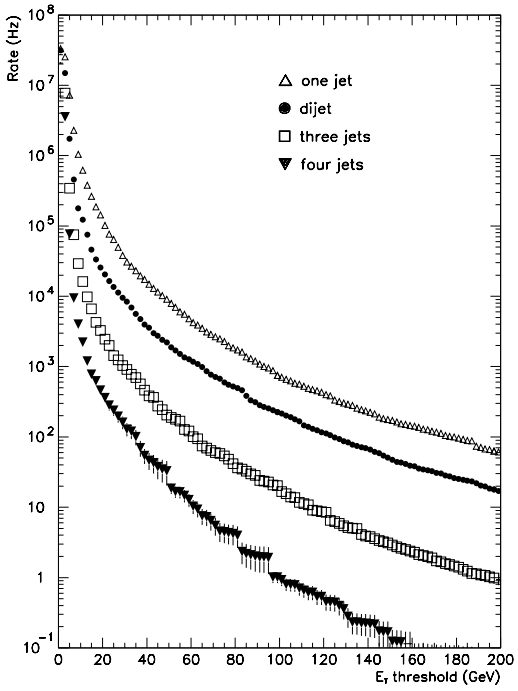

Figure 8: Jet trigger rates at low luminosity.

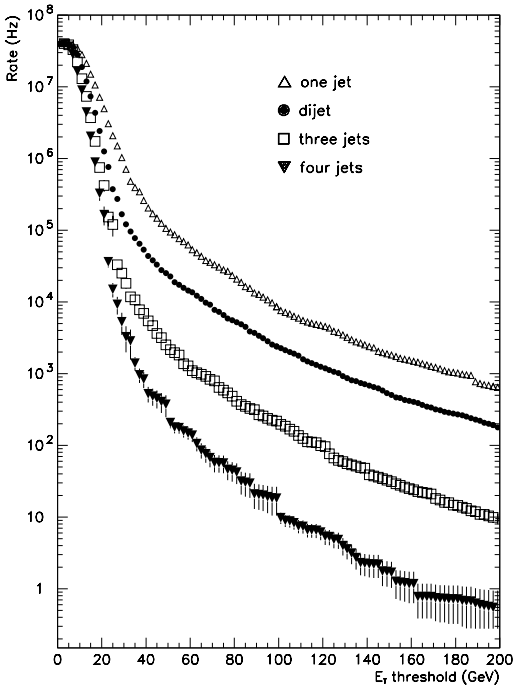

Figure 9: Jet trigger rates at high luminosity.

have been added to each dijet event. Here, the effect of the minimum-bias pile-up is very important for trigger thresholds below about 50 GeV/c. The addition of the pile-up events takes into account the fact that a trigger may come from the minimum-bias pile-up instead of from the dijet event under consideration; in this way, the trigger rates are correctly estimated down to the lowest trigger thresholds, where they saturate below the 40 Mhz bunch-crossing rate.

Missing-E_t triggers are shown in Fig. 10 for low and high luminosity. The background in the missing-E_t trigger at lower values of missing-E_t is due to fluctuations in the energy deposits and cracks in the apparatus. For higher-values of missing-E_t, most of the rate is due to weakly-interacting particles (muons and neutrinos). Missing-E_t is an important signature for SUSY events. Depending on the SUSY parameters, SUSY production cross sections could be as high as 1 nb (1 Hz at 10^{33} /cm^2/s). Other signatures for inclusive SUSY events are the total scalar E_t (sum of $|E_t|$) or the effective mass, equal to the total E_t plus the missing-E_t.

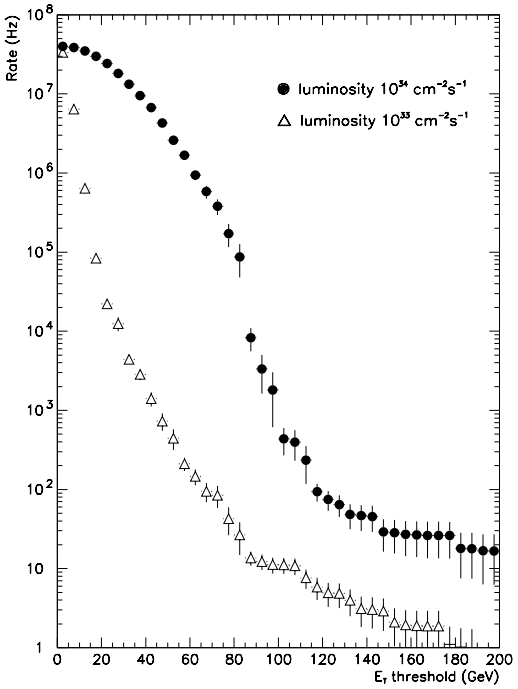

Figure 10: Missing-E_t at low and high luminosity.

4.5 Single charged hadron and tau triggers

The trigger menu should also include single charged hadrons. The most important known source of single charged hadrons is the decay of τ leptons: $\tau^- \rightarrow \pi^- \nu$ (B.R. 11%) and $\tau^- \rightarrow K^- \nu$ (B.R. 0.7%). Heavy vector bosons (W, Z, W′, Z′) decay equally into electrons, muons, and taus (lepton universality), whereas Higgs bosons decay preferentially into taus because of the large tau mass. Half of the tau decays have a single charged hadron, and another 15% have three charged hadrons. The principal hadronic decay modes of the tau lepton are:

$\tau^- \rightarrow h^- \nu$	12%
$\tau^- \rightarrow h^- \pi^0 \nu$	26%
$\tau^- \rightarrow h^- \pi^0 \pi^0 \nu$	10%
$\tau^- \rightarrow h^- h^- h^+ \nu$	10%
$\tau^- \rightarrow h^- h^- h^+ \pi^0 \nu$	4%

Tau trigger algorithms take advantage of the fact that the tau jets are narrow compared to other jets. One third of the hadronic decays can be selected with minimum background by requiring a match between the energy in the calorimeter and the P_t of the (one or three) charged tracks.

5 TRIGGER MENUS

Full trigger menus for low luminosity will be presented in this lecture. These trigger menus are based on the ATLAS physics requirements. They are ‘toy’ menus, intended as an existence proof; the final allocation of trigger bandwidth will be made just before data taking begins. Estimated rates will be given for each of the trigger items. Options for the boundary between Level-2 processing and Level-3 processing will be discussed, especially in what concerns B physics, b-jet tags, and missing-E_t. There will also be a short discussion of the possible use of neural networks in the LHC triggers.

5.1 Evolution of LHC luminosity and physics goals with time

The LHC luminosity will start at a low value (initially perhaps as low as 10^{32} /cm^2/s) and increase slowly up to the design value of 10^{34} /cm^2/s. One possible scenario for the evolution of the time-averaged luminosity consistent with current thinking would be as follows [2]:

2006	$L_{avg} = 2 \times 10^{32}$ /cm^2/s
2007-2008	$L_{avg} = 1 \times 10^{33}$ /cm^2/s
2009-2010	$L_{avg} = 5 \times 10^{33}$ /cm^2/s

The number of pile-up events (minimum bias background) will increase from 2.3 per bunch-crossing at 10^{33} /cm^2/s to 23 per bunch-crossing at 10^{34} /cm^2/s.

The physics goals and the trigger conditions will change as the luminosity increases. But the trigger rates at low luminosity will not be much lower than the rates at standard luminosity, because the physics goals will expand to fill the available bandwidth. More correctly, the physics goals at higher luminosity will be concentrated on more narrow physics objectives because of the rate limitations and the higher background (pile-up).

The main advantage of higher luminosity is the ability to observe high-mass objects with low cross sections. Typically, the cross-section above threshold for a massive object decreases as the fourth power of the mass, so increasing the luminosity by a factor 10 increases the mass reach for high-mass objects such as W′ and Z′ by about 75%.

5.2 Trigger strategy

In developping a trigger for a ‘discovery’ experiment such as LHC, ‘toy’ trigger menus are used to explore the compatibility of the trigger design and the physics goals. These exploratory trigger menus will certainly be different from the trigger menus used in the actual data taking. The duty of the trigger group is to develop a set of tools - ‘handles and knobs’ - that will be available for use in the experiment. These tools should be designed to cover as many physics signatures as possible. The allocation of bandwidth among the possible trigger menu items should be made just before the beginning of data taking, depending on the evolution of the physics goals and on the actual trigger rates measured when beam arrives.

Loose, redundant triggers are needed in order to evaluate backgrounds and determine trigger efficiencies. Newly discovered objects should be observed in as many decay modes as possible, in order to confirm the original discovery and measure cross-sections and branching ratios. Upper limits also contribute to our understanding. Not all of these results require a five standard-deviation ‘discovery’ data sample.

The trigger should be designed for flexibility. Candidates for new physics discoveries should be logged to permanent storage whenever possible, even if current attempts to analyze simulated data fail. Put the events on tape now, and analyze them later, when the data are better understood. For many physics channels, the best data may well be the data we take in the first few years when the luminosity is low.

The Level-1 trigger is a hardware trigger; the trigger parameters (thresholds, isolation criteria, etc.) can be adjusted, but the functionality is limited and fixed. The Level-1 trigger conditions should be loose and inclusive. The Level-1 trigger can nonetheless set flags to guide the higher-level algorithms. The RoIs in the ATLAS trigger are an example of the information that can be passed to the Level-2 trigger. The RoIs that contributed to the Level-1 trigger decision are passed on to Level 2, but additional RoIs with lower thresholds can also be sent to Level 2, along with global event parameters such as missing-E_t and total scalar E_t.

The higher-level algorithms are typically performed on general-purpose commercial processors; they have access to all of the event data and all of the calibration and alignment constants. Nonetheless, Level-2 algorithms generally use only a small part of the data, whereas the Level-3 algorithms use the full event data. ATLAS intends to use special trigger code at Level 2 and a form of the off-line code at Level 3. CMS uses off-line code, pulling data from the event buffers as required to form objects for the execution of high-level object-oriented algorithms.

The trigger items typical of high-luminosity operation depend on high-P_t trigger objects such as leptons, jets, or missing-E_t. High-P_t objects are important for the physics because they signal the presence of high-mass objects, including Z, W, and top, but also most of the anticipated signals for

new physics discoveries. High P_t is important for the selection process, because the high-P_t objects stand out above the minimum-bias background.

At low luminosity, where the high-P_t event rates are small and there is little minimum-bias pile-up, the physics menu can be expanded to include low-P_t physics objectives such as B physics. LHC-B is designed specifically for B-physics studies at low luminosity, with particle-identification to isolate decay modes involving charged pions and kaons. ATLAS and CMS will cover some of the B-physics topics - CP-violation, mixing, and some rare decays - with their general-purpose detectors.

5.3 Standard trigger menus

The symbols used to designate the ATLAS trigger menus are shown in Table 1.

Table 1: Nomenclature for ATLAS trigger objects.

Trigger object	E_t threshold	Conditions	LVL1 object	LVL2 object
$\mu^{\pm}$	6 GeV	none	MU6	mu6
$\mu^{\pm}$	6 GeV	isolation		mu6I
EM cluster	80 GeV	none	EM80	em80
gamma	15 GeV	isolation		g15I
$e^{\pm}$	20 GeV	isolation		e20I
$\tau^{\pm}$	80 GeV	none	TAU80	tau80
$h^{\pm}$	80 GeV	isolation		h80I
jet	100 GeV	none	J100	j100
jet	15 GeV	B vertex		b15
missing-E_t	100 GeV	none	ME100	me100
scalar-E_t	500 GeV	none	SE500	se500
total-E_t	1000 GeV	none	TE1000	te1000

A typical Level-1 trigger menu for low luminosity is shown in Table 2 [3,25]. The first-level trigger for B-physics candidates requires a non-isolated muon with $P_t > 6$ GeV/c.

Table 2: Typical Level-1 trigger menu at low luminosity.

Trigger Menu Item	Rate
MU6	8000 Hz
EM80	200 Hz
EM20I	10000 Hz
EM15I + EM15I	2500 Hz
TAU80	5000 Hz
J100	8000 Hz
J50 + J50 + J50	3000 Hz
ME100	2000 Hz
SE500	1000 Hz
Total Level-1 Trigger Rate	39700 Hz

Some of the flags set at Level 1 to guide the Level-2 algorithms are shown in Table 3. Most of these flags indicate the presence of low-P_t jets. For selected events, the low-P_t jets will be considered as b-jet candidates to be confirmed using the b-jet vertex tag.

Table 3: Typical Level-1 trigger flags at low luminosity.

Level-1 Trigger Flag	Rate	Conditions

MU6	**8000 Hz**	
MU20	400 Hz	
MU20 + MU6	100 Hz	
MU20 + MU20	20 Hz	
MU20 + EM15I	40 Hz	
MU20 + TAU40	400 Hz	
MU20 + n × J15	400 Hz	n > 0, <n> = 3.5
MU20 + J40 + J40	40 Hz	
MU6 + EM15I	800 Hz	
MU6 + MU6	400 Hz	
MU6 + MU6 + MU6	20 Hz	
MU6 + MU6 + EM15I	40 Hz	
MU6 + EM15I + EM15I	40 Hz	
MU6 + n × J15	6000 Hz	n > 1, <n> = 4.5
MU6 + MU6 + J15 + J15	400 Hz	
EM80	**200 Hz**	
EM80 + J100	20 Hz	
EM80 + EM80	30 Hz	
EM20I	**10000 Hz**	
EM20I + TAU40	3000 Hz	
EM20I + n × J15	10000 Hz	n > 0, <n> = 3.5
EM20I + J40 + J40 + J40	200 Hz	
EM20I + J40 + J40 + n × J15	700 Hz	n > 1
EM201 + J100 + J100	250 Hz	
EM15I + EM15I	**2500 Hz**	
EM15I + EM15I + EM7I	1000 Hz	
EM15I + EM15I + J15 + J15	2500 Hz	
TAU80	**5000 Hz**	
TAU150	1000 Hz	
TAU80 + TAU80	800 Hz	
J100	**8000 Hz**	
J200	250 Hz	
J100 + J100	2000 Hz	
J150 + J150	500 Hz	
J100 + J100 + ME100	300 Hz	
J100 + J100 + J100	200 Hz	
J100 + n × J15	4000 Hz	n > 2
J50 + J50 + J50	**3000 Hz**	
J50 + J50 + J50 + J50	600 Hz	
J50 + J50 + J50 + J50 + J50	100 Hz	
J50 + J50 + J50 + J50 + J50 + J50	20 Hz	
ME100	**2000 Hz**	
ME150	30 Hz	
SE500	**1000 Hz**	
SE1000	1 Hz	
Total Level-1 Trigger Rate	39700 Hz	

A Level-2 trigger menu for low luminosity is shown in Table 4. The B physics algorithms are included with the high-P_t menu items. Neither b-jet tags nor missing-E_t recalculations are included in these 'standard' Level-2 trigger menus.

Table 4: Standard Level-2 trigger menu at low luminosity.

Level-2 trigger item	**Rate**
mu40	25 Hz
mu20I	20 Hz
mu20 + mu20	5 Hz
mu20 + j15 + j15 + j15	50 Hz
mu15I + e15I	1 Hz
mu6I + mu6I	10 Hz
mu6I + e15I	9 Hz
e15I + e15I	8 Hz
mu6I + j15 + j15	200 Hz
e80	20 Hz
g40I	60 Hz
e20I	200 Hz
g15I + g15I	100 Hz
tau150	200 Hz
tau100I + tau100I	5 Hz
h80I	2 Hz
j500	1 Hz
j400 + j400	1 Hz
j200 prescale/100	1 Hz
j150 + j150 prescale/100	1 Hz
j100 + j100 + ME100	80 Hz
j100 + j100 + j100 + j100	2 Hz
j100 + j15 + j15 + j15	500 Hz
j50 + j50 + j50 + j50	200 Hz
ME150	30 Hz
SE1000	1 Hz
SUM of LVL2 triggers (except B-physics)	1732 Hz
B-PHYSICS TRIGGERS	
mu6 + e1 + e1 + M(J/ψ)	24 Hz
mu6 + mu5 + mu3	8 Hz
mu6 + e5 + mu3	8 Hz
mu6 + h6 + h6 + M(B)	5 Hz
mu6 + h1.5 + h1.5 + h1.0 + M(φ^0) + M(D_s)	50 Hz
mu6 + mu5 + M(B)	3 Hz
SUM of all B-physics triggers	98 Hz
TOTAL LEVEL-2 TRIGGER RATE	1830 Hz

5.4 B-physics: sequential processing scheme

The ATLAS strategy for the selection of B-physics candidates involves an exceptional use of a sequential selection scheme at Level 2 [3]. The Level-1 trigger rate for muons with $P_t > 6$ GeV/c and $|\eta| < 2.5$ is about 8 kHz at low luminosity (10^{33} /cm^2/s). At Level 2, the precision muon chambers and

the inner tracker can be used to eliminate background and sharpen the P_t cut; this reduces the rate to 4 kHz, including 2 kHz of B decays. The inner tracker can then be used to find candidates for specific B decays of particular interest. All tracks above 1 GeV/c are found in a TRT full scan, and they are identified as muons, electrons, or hadrons using data from the TRT and the calorimeter. Mass cuts are used to improve the selection, as shown in Table 4. The execution time for the TRT full scan is estimated to be about 50 ms. The sequential processing scheme reduces the number of candidates for this time-consuming algorithm.

5.5 Extended higher-level trigger menus

The 'extended' higher-level trigger menus include b-jet tags and recalculation of the missing-E_t for selected events. The ambiguity between 'standard' Level-2 trigger menus and 'extended' trigger menus applies to the present status of the ATLAS trigger design. In CMS, all of the higher-level algorithms (standard or extended) are executed in a single processor, with data transferred to the processor only as needed for the execution of the algorithms.

In ATLAS, several options are under study for the higher-level triggers. In the 'local/global' processing scheme described in the ATLAS Technical Proposal [3], the Level-2 feature extraction is performed in parallel in separate processor farms for each of the detector systems; in this case, the complex 'extended' algorithms would find their place at Level 3. In the 'single-farm' option, on the other hand, data are pulled from the buffers as needed, and 'standard' and 'extended' algorithms could be performed in the same processor [15,26].

There are two advantages to performing the b-jet tags for selected events in the Level-2 processors: the data transfer bandwidth and the processing time. Processing at Level 2 requires only RoI data and uses specially optimized code, whereas processing at Level 3 requires transfer of the full event data and uses the off-line code.

The missing-E_t must be recalculated at Level 2 or at Level 3 to improve the resolution for $W \rightarrow e + \nu$ selection and for certain channels involving tau decays. Missing-E_t calculations present a special problem for Level-2 processing because they require data from all of the calorimeter ROBs. Once again, the problem can be resolved by preselecting events for this algorithm. The data volume is about the same as for the full TRT scan, but the execution time for the missing-E_t calculation is negligible. The data volume required is about 16 kB at Level 2 or about 1 MB at Level 3. It is clear that the missing-E_t should be recalculated at Level 2 for a selected sample of events.

5.6 Neural networks in LHC triggers

Neural networks have been used in some trigger designs to select events of interest by assigning a probability to different possible interpretations of the event. This method can be particularly interesting if the cuts normally used to select event candidates are not orthogonal. On the other hand, the method can be dangerous if the 'training sample' misrepresents the characteristics of the interesting events. Therefore, neural networks are not ususally used at the trigger level. Off-line, neural networks can be used to look for signals from new physics, with the restriction that any signal found should be confirmed by a thorough study of the full data sample.

6. TRIGGER MODELLING

Trigger modelling can be used to determine the influence of different trigger strategies on physics performance and on cost. This lecture will describe a 'paper model' technique which uses full trigger menus, but takes (estimated) average values for parameters such as data transfer volumes and rates, algorithm execution times, and processing overheads. The 'paper model' results can be used to guide the full modelling studies and switching-network emulation. Sequential and parallel processing schemes will be compared, as well as single-farm and multiple-farm architectures.

6.1 Full computer modelling

ATLAS has developed a modelling tool called SIMDAQ [28] based on the commercial object-oriented simulation language MODSIM II [29]. Objects can be built to represent the data acquisition components of the trigger system, and methods can be built to allow these objects to interact with

each other. Full modelling of the trigger system can be performed using data files produced from GEANT simulations of the ATLAS detector. Data files corresponding to the dominant dijet background can be run to measure the overall trigger performance in terms of maximal trigger rates and data volumes. Additional data files corresponding to specific physics channels can also be run in order to investigate efficiencies and extreme running conditions.

Modelling studies will be only as good as the parameters used in the model. Benchmarking of trigger algorithm execution times and hardware and software performance are needed to provide these critical parameters. Technological evolution has to be taken into account on long-term projects such as the LHC. The CPU power available at constant cost has doubled every 18 months for the last 20 years or so, and this evolution is expected to continue for the next 5 years at least [30]. System performance must be extrapolated to the estimated 'date of purchase'.

6.2 Simple 'paper models' for initial optimization

Modelling results have been obtained which are in good agreement with recent laboratory measurements [31]. It is difficult, however, to vary the parameters to test architectural options and to take account of technological advances because of the time necessary to set up the simulation models and because of the long MODSIM execution times.

A 'paper model' approach has been developed in order to obtain crude modelling results without waiting for full modelling studies [32]. Paper models are the next step after 'back-of-the-envelope' calculations. They require a simplified model of the process under study and a complete set of parameters: trigger rates, data volumes and transfer rates, execution times, and overheads. An iterative process should be used to optimize the overall system performance.

The data in the readout buffers should be formatted and ordered to simplify the task for Level-2 processing. With foresight, some of the processing required for Level 2 can be performed in the frontend electronics or in the readout driver modules. In the best-case hypothesis, we estimate that data handling will account for about 50% of the Level-2 processor occupation. If the data is poorly organized, data transfers and execution times could be greatly increased. Note that preprocessing in the ROB modules might also be used to prepare data formats for the Level-2 processors. Figure 11 shows a model for the distribution of the ATLAS data into different readout buffers in the case of a single-farm architecture.

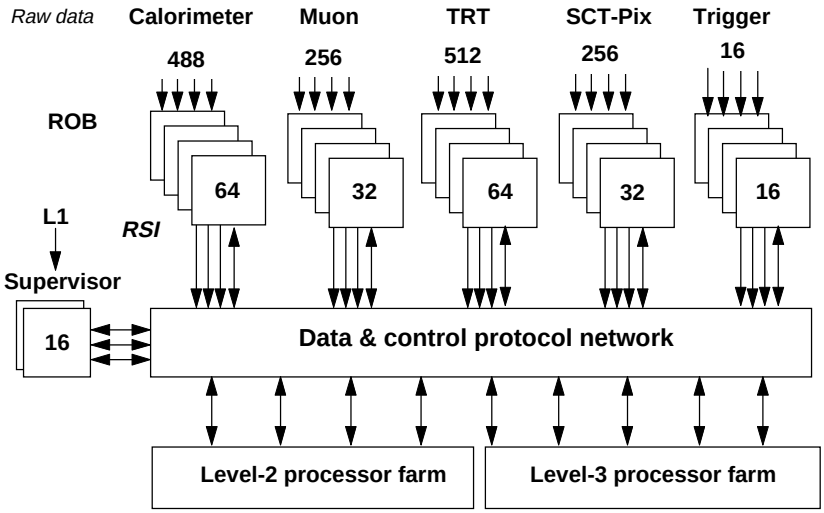

Figure 11: ATLAS Level-2 readout in a single-farm model.

With a 100 kHz input rate, and about 1000 processors, the average Level-2 execution time must not exceed 10 ms. Nonetheless, a small fraction of the events can take much longer. Estimated execution times for Level-2 trigger algorithms, extrapolated to 500-MIPS processors, are shown in Table 5 [32]. Confirmation of the Level-1 trigger objects in the calorimeter and muon systems is very rapid, requiring no more than 100 μs. Tracking algorithms are considerably longer, about 1 ms per RoI. Full TRT scans and b-jet tags are in the range of 100 ms, well beyond the average available

execution time of 10 ms, so these algorithms can be applied only to a small fraction of the events passing Level 1.

Table 5: Feature extraction execution times.

Trigger	system	processing
muon trigger	MUON	100 μs
e/γ/τ trigger	CALO	100 μs
jet trigger	CALO	100 μs
track	TRT	600 μs
track	SCT	800 μs
TRT scan $L=10^{33}$	TRT	50 ms
TRT scan $L=10^{34}$	TRT	200 ms
missing-E_t	CALO	100 μs
B jet tag	SCT	250 ms

6.3 Event processing

The main steps in the event processing in a 'pull' architecture are the following:

1. Send Level-1 data to Level 2
2. Assign Level-2 processors
3. Request data from ROBs
4. Preprocess data in each ROB
5. Send preprocessed data to Level 2
6. Execute feature extraction algorithms
7. Test compatibility with Level-2 trigger

Repeat steps 3 to 7 as required for other detector systems or RoIs

8. Test global Level-2 trigger conditions
9. Send Level-2 decision to supervisor
10. Broadcast Level-2 decision to ROBs

In the case of a Level-2 ACCEPT

11. Send event data to Level-3 processors
12. Execute Level-3 algorithms
13. Send Level-3 decision to supervisor

For each of these main processing steps, the occupation time of each of the hardware systems - supervisor, ROB, busses, interfaces, switching network, processors - should be tabulated. The occupation time for a single RoI depends on the number of ROBs and the number of ROB interfaces for that RoI, the quantity of RoI data, and the preprocessing and feature-extraction execution times. The occupation times are calculated in the 'paper' models using average values for these parameters. The total occupation (and the total latency) for each of the hardware systems can be found by summing over all processing steps for each RoI type and each detector system.

6.4 Occupation and latency

The trigger menu must be used to determine the number of data requests and the number of RoIs for each RoI type and for each detector system. For the sequential event selection scheme, the rejection factor obtained at each processing step must be taken into account. The numbers obtained for the ATLAS low-luminosity trigger [25] are shown in Table 6. These are the only numbers required to determine the occupation of the hardware systems and the overall latency in the simple 'paper' model discussed here.

Table 6: Summary of rates for sequential ATLAS trigger at low luminosity.

Algorithm	System	Data Requests	RoI numbers
muon	muon	8000 Hz	8420 Hz
EM cluster	calorimeter	22940 Hz	30372 Hz
track	TRT + silicon	7200 Hz	7599 Hz
full track scan	TRT	4000 Hz	4000 Hz
full track scan	silicon	2000 Hz	20000 Hz
jet	calorimeter	10202 Hz	19068 Hz
b-jet tag	silicon	1062 Hz	2161 Hz
missing-E_t	calorimeter	835 Hz	835 Hz

6.5 Comparison of processing strategies

Parallel and sequential processing schemes can be evaluated by simply comparing the rate summary for sequential processing in Table 6 with the rate summary for parallel processing shown in Table 7 [32]. The number of tracking RoIs and the number of jet RoIs that have to be processed for the standard Level-2 trigger menu are reduced by a factor four when sequential processing is used. Nonetheless, either parallel or sequential processing of these RoIs is compatible with the processing power available at Level 2. On the other hand, b-jet tags and missing-E_t calculations in the extended trigger menus can only be processed at Level 2 in the sequential processing option, which reduces the number of b-jet candidates by a factor of about 30 and the number of missing-E_t calculations by more than a factor 10.

Table 7: Summary of rates for parallel processing of ATLAS trigger.

Algorithm	System	Data Requests	RoI numbers
muon	muon	8000 Hz	8420 Hz
EM cluster	calorimeter	25700 Hz	34690 Hz
track	TRT + silicon	33700 Hz	43110 Hz
full track scan	TRT	8000 Hz	8000 Hz
full track scan	silicon	8000 Hz	NA
jet	calorimeter	24980 Hz	82420 Hz
b-jet tag	silicon	20500 Hz	73820 Hz
missing-E_t	calorimeter	14030 Hz	14030 Hz

The main argument in favor of the sequential processing option is flexibility. The b-jet tag and the missing-E_t calculation are two examples in favor of sequential processing. The full track scan required for B physics is another. We don't know how to treat the B-physics candidates in a fully-parallel scheme, because the algorithm requires that new RoIs found in the TRT scan be further analyzed in the calorimeter and silicon systems. It is not possible to treat these systems in parallel. On the other hand, the b-jet tags and the missing-E_t calculations could eventually be performed at Level 3, but at greater cost in processing power and data-transfer bandwidth. The resources needed when the standard algorithms are processed at Level 2 and the b-jet tags and the missing-E_t are processed at Level 3 are shown in Table 8. Note that the RSIs are over-saturated in this particular model.

Table 8: Total occupation for Level 2 plus minimal Level 3, with b-jet tags and missing-E_t at Level 3.

LVL1 trigger rate	34270 Hz		
LVL2 + LVL3 latency	52.3 ms	(average for all LVL1 events)	
Buffer length required	1793.2 events	(LVL2 + LVL3 buffers)	
Hardware element	**# required**	**# in model**	**Occupation**
ROB	331.4	768	43.2 %
RSI bus	29.9	192	15.6 %
RSI	213.0	192	110.9 %
ATM (data)	127.6	192	66.5 %
ATM (control)	3.0	192	1.6 %
SFI	121.0	192	63.0 %
SFI bus	27.5	192	14.3 %
processors	1488.0	2650	56.2 %

The resources needed when all of the event selection algorithms, including b-jet tags and missing-E_t are processed at Level 2 are shown in Table 9. The number of processors required is reduced by about 700 500-MIPS units, and the load on the switching network is reduced by a factor five.

Table 9: Total occupation for Level-2 plus minimal Level-3 processing, with all selection at Level 2.

LVL1 trigger rate	34270 Hz		
LVL2 + LVL3 latency	27.3 ms	(average for all LVL1 events)	
Buffer length required	934.2 events	(LVL2 + LVL3 buffers)	
Hardware element	**# required**	**# in model**	**Occupation**
ROB	370.9	768	48.3 %
RSI bus	8.1	192	4.2 %
RSI	138.1	192	71.9 %
ATM (data)	24.0	192	12.5 %
ATM (control)	3.3	192	1.7 %
SFI	42.5	192	22.1 %
SFI bus	5.3	192	2.8 %
processors	796.0	2650	30.0 %

6.6 Documentation

All of the knowledge obtained from these different studies should be documented in trigger requirements documents and design reports. The responsibilities of the trigger group and the interfaces between the trigger system and other systems should be clearly defined in a Global Users' Requirements Document. The objectives of the trigger system - what we want it to do - should be described in the Trigger Users' Requirements Document. The design - how we intend to build it - should be described in the System Requirements Document. The sharing of responsibilities between participating groups should be clearly defined and well-matched to the resources available. These documents should evolve as our understanding of the problem increases. Some objectives will be mutually exclusive due to the eternal trade-off between cost and performance. The requirements, the design, and the responsibilities should be subject to regular reviews, both internal and external. All of these aspects should be described in detail in the Technical Design Report.

7. CONCLUSIONS

This lecture series has attempted to describe some of the steps required in the design of a trigger system for experiments such as those planned for the LHC. Trigger design must be based on the

physics goals of the experiment - the so-called ‘top-down’ approach. The trigger architecture must be sufficiently flexible to allow the trigger to follow the evolution of the physics goals as well as the technological evolution - especially for long-term projects such as the LHC. The trigger menus for general-purpose experiments like ATLAS and CMS should ensure a broad physics reach, with exclusive and inclusive trigger items corresponding to a full spectrum of possible signatures for new physics. The trigger design should proceed from simple calculations, through ‘paper’ models, then on to demonstrators, emulators, and full modelling studies. Requirements and responsibilities should be documented at an early stage to avoid uneconomic use of human and financial resources.

REFERENCES

1. The LHC Study Group, “The Large Hadron Collider Conceptual Design”, CERN/AC/95-05 (1995).

2. J. Gareyte, “LHC Performance During Running-in”, SL/Note 93-06 (1993).

3. ATLAS Technical Proposal, CERN/LHCC/94-43 (1994).

4. CMS Technical Proposal, CERN/LHCC/94-38 (1994).

5. LHC-B Letter of Intent, CERN/LHCC/95-5 (1995).

6. ALICE Technical Proposal, CERN/LHCC/95-71 (1995).

7. D. Kotlinski and C. Racca, “B-physics Performance of the CMS Detector”, Beauty ‘95 (Oxford), Nucl. Instr. and Meth. A 368 (1995) 115.

8. A. Nisati, “B-physics in ATLAS”, Beauty ‘95 (Oxford), Nucl. Instr. and Meth. A 368 (1995) 109.

9. P. Eerola, et al., “B Physics in ATLAS”, ATLAS Internal Note PHYS-NO-41 (1994).

10. M. Smizanska, “Second Level TRT Trigger for B Physics”, ATLAS Internal Note PHYS-NO-89 (1996).

11. S. Erhan, “LHC-B: a Dedicated LHC Collider Beauty Experiment”, Beauty ‘95 (Oxford), Nucl. Instr. and Meth. A 368 (1995) 133.

12. ATLAS Letter of Intent, CERN/LHCC/92-4 (1992).

13. E. Richter-Was, et al., “Minimal Supersymmetric Standard Model Higgs rates and background in ATLAS”, ATLAS Internal Note PHYS-NO-74 (1996).

14. LHC-B Trigger and Data Acquisition Group, “LHC-B Trigger and Data Acquisition Progress Report”, LHCB 97-005 (1997).

15. P. Le Du, IEEE/NSS, Anaheim CA (1996); J. Bystricky, et al., “A Sequential Processing Strategy for the ATLAS Event Selection”, ATLAS Internal Note DAQ-NO-59 (1996).

16. J. Bystricky, “Jet Trigger Rates from Fast Simulations”, ATLAS Internal Note DAQ-NO-29 (1995).

17. E. Barberio, et al., “Implementation of the First Level Muon Trigger”, ATLAS Internal Note DAQ-NO-39 (1994).

18. G. Ambrosini, et al., “A Proposal for the ATLAS Level-2 Muon Trigger in the Barrel Region”, ATLAS Internal Note MUON-NO-61 (1995).

19. I. Brawn, et al., “First-Level Trigger System for LHC Experiments”, RD-27 Status Report, CERN/DRDC 93-32 (1993).

20. J.R. Hubbard, “The ATLAS Trigger/DAQ System”, Nucl. Instr. and Meth. A 360 (1995) 331.

21. S. Dasu, “Calorimeter Trigger Electronics for CMS Detector at LHC”, CHEP97 (B164), Berlin (1997).

22. I. Brawn, et al., “The Level-1 Calorimeter Trigger System for ATLAS”, ATLAS Internal Note DAQ-NO-30 (1995).

23. J. Bystricky, et al., “ATLAS Trigger Performance: Electron/Photon Triggers at Level 2”, ATLAS Internal Note DAQ-NO-28 (1995).

24. ATLAS Trigger Performance Working Group, “Trigger Algorithms in ATRIG Version 1.30”, ATLAS Internal Note DAQ-NO-60 (1996).

25. J. Bystricky, et al., “ATLAS Trigger Menus at Luminosity 10^{33} /cm^2/s”, ATLAS Internal Note DAQ-NO-54 (1996).

26. Z. Hajduk, et al., “Modelling of Local/Global Architectures for Second Level Trigger at the LHC Experiment”, ATLAS Internal Note DAQ-NO-13 (1994).

27. E. Barberio, et al., “Implementation of the First Level Muon Trigger”, ATLAS Internal Note DAQ-NO-39 (1994).

28. C. Hortnagl and S. Hunt, “SIMDAQ Users Guide”, ATLAS Internal Note DAQ-NO-41 (1995).

29. CACI Products Company, “MODSIM II - The Language for Object-Oriented Programming” (1993).

30. S. Levin, “PCs: Facts, Figures, and Forecasts”, CHEP97, Berlin (1997).

31. J. Vermeulen, et al., “Discrete-event Simulation of Second-level Triggering in ATLAS”, submitted to RT97, Beaune (1997).

32. J. Bystricky, et al., “A Model for Sequential Processing in the ATLAS LVL2/LVL3 Trigger”, ATLAS Internal Note DAQ-NO-55 (1996).